

NTrack: A Multiple-Object Tracker and Dataset for Infield Cotton Boll Counting

Md Ahmed Al Muzaddid[✉] and William J. Beksi[✉], *Member, IEEE*

Abstract—In agriculture, automating the accurate tracking of fruits, vegetables, and fiber is a very tough problem. The issue becomes extremely challenging in dynamic field environments. Yet, this information is critical for making day-to-day agricultural decisions, assisting breeding programs, and much more. To tackle this dilemma, we introduce *NTrack*, a novel multiple object tracking framework based on the linear relationship between the locations of *neighboring* tracks. *NTrack* computes dense optical flow and utilizes particle filtering to guide each tracker. Correspondences between detections and tracks are found through data association via direct observations and indirect cues, which are then combined to obtain an updated observation. Our modular multiple object tracking system is independent of the underlying detection method, thus allowing for the interchangeable use of any off-the-shelf object detector. We show the efficacy of our approach on the task of tracking and counting infield cotton bolls. Experimental results show that our system exceeds contemporary tracking and cotton boll-based counting methods by a large margin. Furthermore, we publicly release the *first* annotated cotton boll video dataset to the research community.

Note to Practitioners—This work is motivated by the need to provide highly-accurate estimates of the total number of cotton bolls across an entire farm. We provide a multiple object tracking framework for automating the counting process using a dynamic motion model that can reidentify severely occluded objects. This information is immensely beneficial to agronomists and breeders. For example, it can allow them to accelerate the selection of genotypes and identify cotton cultivars that exhibit tolerance to adverse environmental conditions (e.g., drought, poor soil quality, etc.) via yield prediction. Since the performance of our tracker is tied to the accuracy of the object detector, the ability to swap detectors is important for enhancing the usability of the system. Our dataset structure was modeled after similar multiple object tracking datasets for the purpose of increasing adoption among practitioners. To implement our system, it is assumed that the image/video capture device is of high resolution and data is acquired under ideal lighting conditions. The framework can be run on any commercial-off-the-shelf platform (e.g., ground-based robots, unmanned aerial vehicles, etc.), with sufficient computing and memory resources, using a vision-based sensor.

Index Terms—Agricultural automation, computer vision for automation, visual tracking.

Manuscript received 20 September 2023; accepted 30 November 2023. This article was recommended for publication by Associate Editor K. Zhu and Editor G. Fortino upon evaluation of the reviewers' comments. (*Corresponding author: William J. Beksi*).

The authors are with the Department of Computer Science and Engineering, The University of Texas at Arlington, Arlington, TX 76019, USA. (e-mail: mdahmedal.muzaddid@mavs.uta.edu, william.beksi@uta.edu).

Color versions of one or more figures in this article are available at <https://doi.org/10.1109/TASE.2023.3342791>.

Digital Object Identifier 10.1109/TASE.2023.3342791

MULTIMEDIA MATERIAL

The source code, dataset, and documentation associated with this project can be found at <https://robotic-vision-lab.github.io/ntrack>.

I. INTRODUCTION

COTTON (*Gossypium hirsutum* L.) is a vital source of natural fiber. It accounts for nearly 25% of total world textile fiber use [1]. Not only is cotton one of the most important textile fibers in the world, but it has also become a substantial source of food and feed for humans and livestock by providing cottonseed oil and hulls [2]. Improving the production of cotton is essential to fulfilling the fiber, food, and feed requirements of the Earth's increasing population [3]. In addition, cotton is a high-valued crop that requires a significant number of inputs such as preparing seed beds, planting, reducing competition from insects and weeds, applying harvest aids, and harvesting. Therefore, among stakeholders, the high return value and cost of cotton production provides incentives for embracing technologies to improve profitability by reducing expenses and boosting yields [4].

A. Significance of Counting Cotton Bolls

Infield cotton boll counting is *key* to predicting fiber yield as well as providing a better understanding of the physiological and genetic mechanisms of the crop's growth and development. Repeated counting can contribute to the calculation of the growth rate in the flowering and boll maturity stages, and allow for selecting genotypes that more effectively utilize their energy to form cotton products. The standard approach to obtain yield information is by manual field sampling, which is *tedious, labor intensive, and expensive*. Constrained by these limitations, sampling is done over a few separate crops and the measurements are extrapolated over an entire farm. However, inherent human bias and sparsity in the measurements can result in *inaccurate* yield estimation. Improving yield is a primary objective in cotton management projects. Physiological factors and environmental variables all have an effect on flower and boll retention. Understanding these processes is *crucial* not only to enhancing cotton yield, but also to advancing the study of plant phenotyping, i.e., the process of measuring and analyzing observable plant characteristics.

B. Object Detection and Tracking in Agriculture

The last few decades have seen remarkable advances in vision-based object tracking. This research has mainly been

arXiv:2312.10922v1 [cs.CV] 18 Dec 2023

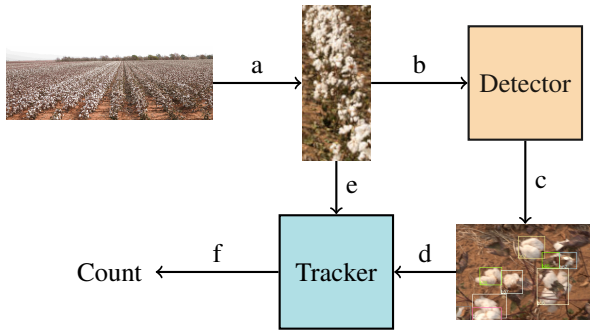


Fig. 1: An overview of NTrack, a multiple object tracking system for infield cotton boll counting. The steps from data collection to cotton boll count estimation are the following: a - capture video, b - extract video frames, c - detect cotton bolls, d - input cotton boll detections to the tracker, e - input video to the tracker, f - output the number of cotton bolls.

applied to tracking pedestrians [5]–[7] and vehicles [8], [9], with benefits to many other important applications such as surveillance, traffic safety, autonomous driving, and more. Nevertheless, vision-based tracking has not evolved proportionally for the agricultural domain. There is a *dire* need for tracking algorithms and datasets to support operations in agriculture. For instance, plant detection and tracking may be utilized to optimize the usage of water, fertilizer, or other chemicals through variable-rate applications. Accurately counting the number of leaves, flowers, fruits, etc., is *vital* for yield prediction and plant phenotyping. Non-destructive, high-throughput data acquisition platforms (e.g., unmanned aerial vehicles, ground-based robots, etc.) are enabling experts to analyze more of this data for optimization.

C. Challenges in Detecting and Tracking Cotton Bolls

Detecting cotton bolls is a *hard* problem and tracking cannot be done if the object detector fails. Bolls are often clustered together and they may be split into two or more disjoint regions by branches, foliage, or other occlusions. In contrast to fruits with rigid shapes (e.g., apples, oranges, etc.), cotton bolls have complex structures and varied sizes [10]. Hence, the ability to detect and provide a highly-accurate count of the total number of cotton bolls in a given field is an *open problem* that we address with our framework, Fig. 1.

The lack of high-quality datasets is a *significant* roadblock for meaningful progress in precision plant phenotyping. Annotated video datasets for cotton crops are *nonexistent*. With the aim of establishing a robust system for tracking and counting cotton bolls, we created **TexCot22** [11], an infield cotton boll video dataset. Each tracking sequence was collected from unique rows of an outdoor cotton crop research plot located in the High Plains region of Texas, Fig. 2. The research plot is comprised of multiple varieties of cotton. Specifically, each row contains the same cultivar of cotton while different rows have unrelated cultivars. This results in a diverse variety of cotton boll shapes and sizes. Additionally, we captured video sequences from rows treated with contrasting levels of irrigation, which has a direct impact on the size and the shape of bolls.



Fig. 2: The cotton crop research field used for data collection.

In summary, our contributions are the following.

- We propose a new tracking system that infers an occluded object’s location based on the visibility of its neighbors, and allows the tracker to maintain identity even under the existence of heavy occlusions.
- We identify limitations in appearance-based re-identification techniques by outperforming the state of the art in many metrics.
- We present the first publicly available infield cotton boll video dataset for advancing vision-based research in precision plant phenotyping.

The remainder of the paper is structured as follows. We explain the object detection and tracking problem, and summarize related research in Section II. In Section III, our detection and tracking system is presented. The details of our infield cotton boll video dataset are provided in Section IV. Section V outlines and discusses the results of our experimental evaluation. We conclude in Section VI and provide directions for future work.

II. RELATED WORK

Detecting and tracking objects is one of the most fundamental tasks in computer vision. Object detection is the process of identifying a target object in an image or a single video frame. Specifically, it is the task of detecting *instances* of objects that belong to a certain class. Object tracking seeks to predict the positions, and other pertinent information, of moving objects in a video. Single-object tracking involves the following steps: (i) detect the location of the object, (ii) assign a unique identification to the object, and (iii) track the object as it moves through the video sequence while storing the relevant information. In multiple object tracking (MOT) [12], given an input video the task is partitioned into locating multiple objects, maintaining their identities, and yielding their individual trajectories. The overall process is shown in Fig. 3.

A. Multiple Object Tracking

MOT approaches can be categorized into *online* and *offline* (batch) tracking. While offline tracking optimizes output based on past and future observations, online tracking only has access to information up until the current frame. Offline methods formalize tracking as an association problem and are solved by using global optimization techniques. For example, early work by Zhang et al. [13] used a probabilistic model to associate detections with tracks by solving an augmented min-cost flow problem. A hierarchical association framework that allows for

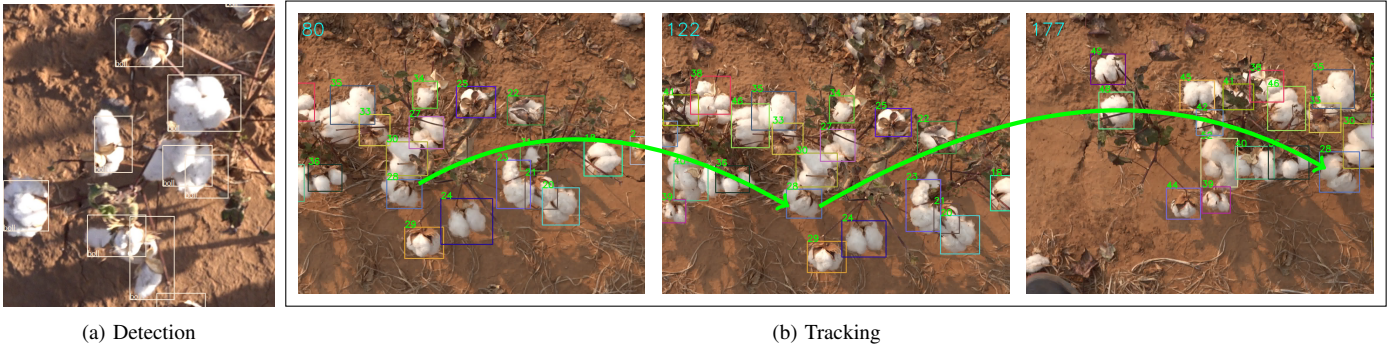


Fig. 3: Multiple object tracking involves (a) detecting the location of objects and placing bounding boxes around them; and (b) associating a unique identification to each object, which is then used to track the trajectories of the objects as they pass through the video sequence.

the integration of affinity measures or optimization methods was put forth by Huang et al. [14]. Yang et al. [15] attempted to find the best global associations and transformed the task of finding these associations into an energy minimization problem.

With limited information, online methods tend to be implemented in a greedy fashion. Currently, the dominant approach for online tracking follows a tracking-by-detection paradigm (e.g., [6], [16]–[18]). When performing tracking-by-detection, an object detector first localizes all objects of interest via a set of bounding boxes. Then, the tracking system associates bounding boxes with preexisting tracks based on motion, appearance, spatial, or other affinities. As a result, object detection accuracy plays a decisive role in the final tracking performance. However, many methods only consider detection boxes whose scores are higher than a set threshold. Objects with low detection scores (e.g., due to occlusions) are discarded, which results in sub-optimal results. Trackers such as ByteTrack [19] try to solve this problem by considering nearly every detection in their association method.

B. Motion Models

Various motion models have been used to estimate spatial affinity including the bounding box intersection over union and Euclidean distance metrics. For instance, to estimate a pedestrian’s velocity, Leal-Taixé et al. [20] introduced an interaction feature encoded from image features based on the pedestrian’s environment. Bewley et al. [21] used a Kalman filter-based motion model to predict track positions while detections are associated via the Hungarian algorithm [22].

To overcome the linearity and Gaussian restriction of the Kalman filter, Okuma et al. [23] utilized a particle filter for tracking. Li et al. [24] used a cascade particle filter, which consists of multiple stages of importance sampling to track objects in low frame rate videos. Optical flow was exploited by Choi [25] to encode the relative motion pattern for estimating the likelihood of matching detections. Yoon et al. [26] considered time-varying multiple relative motion models to represent motion context and facilitate data association. Although these approaches exploit relative motion, their constant velocity motion model is not applicable for many scenarios including ours.

Mauri et al. [27] discussed the use of depth, predicted from monocular images using self-supervised depth estimation [28], to estimate vehicular motion. Unfortunately, coarse depth estimation based on such techniques cannot be used in our situation. These models are not able to distinguish between two cotton bolls at slightly different depths. In our approach, we use an optical flow-based dynamic motion model along with a relative location estimator to update object locations.

C. Appearance Models

Similar to motion models, appearance models are extensively used in MOT. An appearance model extracts re-identification features from image regions corresponding to each bounding box. Appearance-based affinity metrics have proven to be very informative in the presence of long-occlusion intervals. Examples include POI [5], DeepSORT [6], and Tracktor [16], which extract appearance features using deep convolutional neural networks (CNNs). Recent transformer-based approaches (e.g., TrackFormer [29]) also use implicit appearance cues to reidentify objects. More traditional methods have been used too. For instance, region covariance matrices [30], color histograms [31], and gradient-based representations [32], may be leveraged to find appearance-based similarity. In contrast to these works, we propose a relative location-based re-identification technique that can handle significant changes in appearance due to long-spanning occlusions.

D. Multiple Object Tracking in Agriculture

Precisely detecting and tracking objects is imperative for automated fruit/vegetable/fiber counting. In work by Hung et al. [33], apple trees were sampled every 0.5 meters to estimate yield by counting the apples in each non-overlapping image. Chen et al. [34] implemented a two-stage method to count apples and oranges from images. An incremental structure from motion technique was proposed by Roy and Isler [35] to register and localize apples in 3D, which is later used for extracting the count. Häni et al. [36] first identified apple clusters in images based on color, and then used a CNN to classify the clusters where each class represents the number of apples in the cluster. Afonso et al. [37] provided a detection-based approach to enumerate tomatoes in images captured

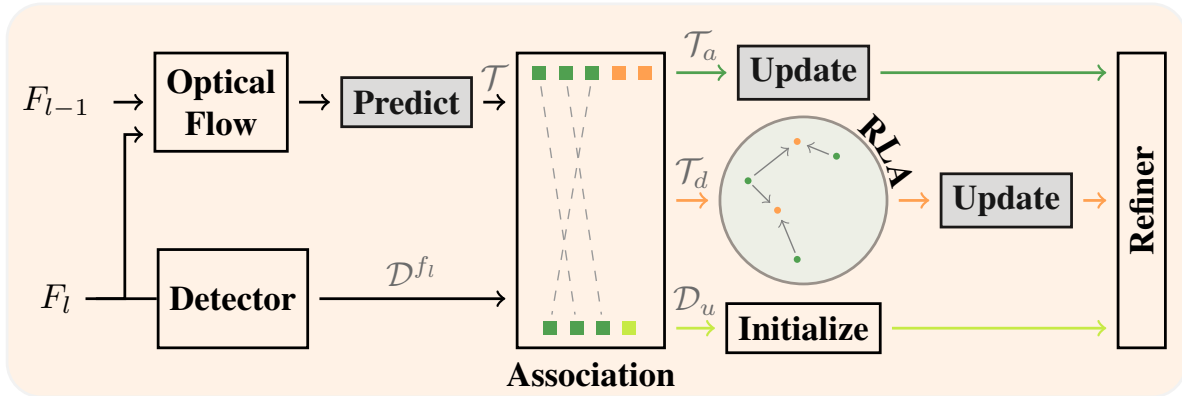


Fig. 4: The NTrack pipeline. The *Association* module finds correspondences between the predicted state of \mathcal{T} tracks (top, green squares). \mathcal{D}^{f_i} is the set of detection bounding boxes (bottom, green squares) detected in frame F_l . The dormant (unmatched) tracks \mathcal{T}_d (orange squares) are analyzed by the *Relative Location Analyzer* (RLA) and updated accordingly. In the RLA module, the dormant tracks’ locations (orange circles) are estimated based on the location of their nearest neighbors (green circles). Unmatched detections \mathcal{D}_u (bottom, light-green squares) are passed through the *Initialize* module as candidates for a new track.

from a greenhouse environment. A DeepSORT inspired tracking method to count fruit in a controlled setting was used by Kirk et al. [38]. All of the aforementioned techniques tally fruits composed of rigid shapes, which are simpler to separate into clusters thus making the counting task easier. On the other hand, counting irregular-shaped cotton bolls under dynamic field conditions is far more challenging.

E. Cotton Boll Counting

To acquire information for yield prediction, recent research has developed algorithms to segment and count cotton bolls. Sun et al. [39] introduced a counting method based on the geometric features of cotton bolls. This was done by applying color and spatial features to segment bolls from the background, followed by geometric feature-based algorithms to estimate the boll count. Tedesco-Oliveira et al. [40] used different deep learning-based object detection models on a cotton crop dataset consisting of 948 images for training, 236 images for validation, and 205 images for testing. By comparison, our dataset is *significantly larger* (see Section IV) and we employ a model that is capable of detecting objects of various sizes. Sun et al. [41] take a 3D approach to counting cotton bolls by using point clouds reconstructed from multi-view images via structure from motion under field conditions.

All of the preceding methods investigate the counting of cotton bolls from images. Image-based counting requires automated or manual sampling. For example, Tedesco-Oliveira et al. [40] selected 25 dissimilar images so that there were no overlapping images in each video sequence. Such sampling-based methods demand additional pre-processing and post-processing steps. Conversely, our approach not only eliminates this overhead without sacrificing accuracy, but it also achieves better accuracy than previous works. Moreover, we argue that counting from videos has the potential to locate additional cotton bolls since the counting sequence enables an automated system to find bolls that may otherwise be occluded in a single image. To the best of our knowledge, our work is the first to engage in the cotton boll counting task *directly from infield video sequences*.

III. APPROACH

The architectural overview of NTrack is depicted in Fig. 4. Similar to other tracking-by-detection systems, the performance of NTrack highly depends upon the detection accuracy. We assume that the detection bounding boxes in every frame are estimated prior to tracking. The tracking procedure is independent of the underlying detection algorithm, which allows NTrack’s *Detector* module to use any state-of-the-art object detection method to identify cotton bolls.

Multiple tracks, each linked to a unique cotton boll and steered/guided by a particle filter, are responsible for estimating the location of an associated boll. The job of the *Association* module is to find the correspondences between detections and tracks based on a matching criteria. Given a track’s past trajectory along with its neighbors’ trajectories, the *Relative Location Analyzer* (RLA) module can estimate the current location of the track. A track is suppressed by the *Refiner* module if the track’s location goes out of the frame border or it cannot be matched against a detection in recent frames.

We denote a set of detections by $\mathcal{D} = \{r_i\}$, where r_i is the detection response represented as the tuple $(x_i, y_i, s_i, w_i, f_i)$. Within the tuple, (x_i, y_i) is the center, s_i is the size, and w_i is the width of the detected bounding box. The frame/time at which an object is detected is defined by f_i . Note that we use f_i to denote both the frame and time interchangeably. $\mathcal{D}^{f_i} \subset \mathcal{D}$ is the set of bounding boxes detected in frame f_i . We define a track $\tau_k \in \mathcal{T}$ over multiples frames by a set of bounding boxes associated with a particular object, where \mathcal{T} represents the set of all tracks in the system. Ideally, each object is associated with a single track. In reality, maintaining a perfect one-to-one mapping between an object and a track is impossible due to occlusions, misdetections, and ambiguous associations. Therefore, a track is *active* in a given frame if the system can successfully associate the track’s predicted bounding box with a detected bounding box, otherwise it is *dormant*.

For each new frame F_l , dense optical flow is computed by the *Optical Flow* module with respect to the previous

frame F_{l-1} based on the Gunnar-Farneback algorithm [42]. Optical flow vectors are outputted for each pixel of the frame. Next, informed by these flow vectors, all tracks predict their new location in frame F_l via the *Predict* module. Each track employs a particle filter for the prediction and update step. The particle filters track the bounding box locations (centers). Nonetheless, since the camera motion and movement of the objects are irregular, neither a constant velocity nor constant acceleration model-based state estimation performs as expected. Hence, we apply a dynamic flow velocity model for the bounding box location estimation. Unlike location, the scale and width of the bounding box changes gradually and is therefore tracked by a Kalman filter using a constant velocity model.

With the detection bounding boxes provided by the tracks, the *Association* module attempts to make a unique correspondence between two sets of bounding boxes. It produces the following outputs: (i) a set of active tracks \mathcal{T}_a successfully matched against detections \mathcal{D}_m , (ii) a set of dormant tracks $\mathcal{T}_d = \mathcal{T} \setminus \mathcal{T}_a$, and (iii) a set of unmatched detections $\mathcal{D}_u = \mathcal{D}^{f_l} \setminus \mathcal{D}_m$. The particle filters associated with the active tracks \mathcal{T}_a update their state using the information from matched detections \mathcal{D}_m through the Association module's *Update* module. The dormant track \mathcal{T}_d 's states are analyzed by the RLA and updated via its *Update* module. If any of the remaining unmatched detections \mathcal{D}_u exceeded a detection confidence threshold, then they are initialized as new tracks (*Initialize* module). Lastly, the *Refiner* module removes any track that was dormant for the last 100 frames.

A. Object Location Prediction

Instead of using well-known motion models to predict the next state (x_i, y_i, s_i, w_i) of the object, we use optical flow-based motion estimation. Due to outdoor environmental conditions (e.g., wind), the branches of a cotton plant can sway back and forth. Moreover, the camera movement over the terrain is erratic, which causes irregular motion dynamics. Even under these adverse conditions, we are still able to find reliable locations of the tracked objects in image coordinates through optical flow. In the prediction step, the particles of the particle filter are moved according to the estimated flow velocities. Since we have multiple targets per frame, we opt for a robust to noise dense optical flow algorithm instead of sparse flow, which would require estimating flow separately for each object.

B. Object Location Update

During the update phase, a track could be in an active or dormant state based on the association outputs. Thus, we use one of two different routines to update a track. If the track is active in frame f_l , then we update the weight of the particles based on direct observation (i.e., the detected object bounding box from the detector). Otherwise, we use the relative locations with respect to the neighboring tracks as indirect observations to update the dormant track. More specifically, the relative locations are used to calculate the bounding box center, which is then used as a proxy for the direct observation in order to update the particle filter.

C. Relative Object Location

Cotton plants in the field may move unpredictably, which makes the tracking task much more difficult. However, the locations of the cotton bolls are not totally independent of each other. In fact, they are highly correlated with neighboring bolls, Fig. 5. More formally, we denote the location (x, y) of a track τ_i in the image coordinate at time f_l as $\rho_{\tau_i}^{f_l} \in \mathbb{R}^2$. The locations along the image width (x) and height (y) are independent, and the estimated location based on the neighbor track τ_j is defined as $\rho_{\tau_i, \tau_j}^{f_l} \in \mathbb{R}^2$. Similarly, we define $d_{\tau_i, \tau_j}^{f_l} \in \mathbb{R}^2$ as the relative distance of track τ_i , with respect to neighbor τ_j , recorded at time f_l . For simplicity, in the following derivation we assume $\rho_{\tau_i}^{f_l}$, $\rho_{\tau_i, \tau_j}^{f_l}$, etc., are scalars and that they represent only the x component of the location. Based on the observed correlation (Fig. 5), we assume that the relative distance between two neighboring tracks changes linearly with the track's location. Concretely, let $d_{\tau_i, \tau_j}^{f_l} = c_1 \cdot \rho_{\tau_j}^{f_l} + c_0$ where c_1 and c_0 are constants. We derive the linear relationship between the locations of two neighboring tracks as

$$\begin{aligned} d_{\tau_i, \tau_j}^{f_l} &= c_1 \cdot \rho_{\tau_j}^{f_l} + c_0, \\ d_{\tau_i, \tau_j}^{f_l} + \rho_{\tau_j}^{f_l} &= c_1 \cdot \rho_{\tau_j}^{f_l} + c_0 + \rho_{\tau_j}^{f_l}, \\ \rho_{\tau_i, \tau_j}^{f_l} &= (c_1 + 1) \cdot \rho_{\tau_j}^{f_l} + c_0, \end{aligned} \quad (1)$$

which suggests that the location of neighboring tracks can be a good estimator of a dormant track's location.

Based on this insight, we calculate track τ_i 's location at time f_l based on a particular neighbor τ_j as follows. Let $\rho_{\tau_j}^{f_l}$ and $\rho_{\tau_i, \tau_j}^{f_l}$ be continuous random variables. The linear relationship between a neighboring track's location implies that we can assume the mean $E[\rho_{\tau_i, \tau_j}^{f_l}]$ is linear in $\rho_{\tau_j}^{f_l}$. At the same time, assuming the variance $var[\rho_{\tau_i, \tau_j}^{f_l}]$ is constant over f_l , we can model $\rho_{\tau_i, \tau_j}^{f_l}$ as a Gaussian random variable

$$\rho_{\tau_i, \tau_j}^{f_l} \sim \mathcal{N}(\mu_{\tau_i, \tau_j}^{f_l}, \sigma_{\tau_i, \tau_j}^2), \quad (2)$$

where

$$\begin{pmatrix} \rho_{\tau_i, \tau_j}^{f_1} \\ \rho_{\tau_i, \tau_j}^{f_2} \\ \vdots \\ \rho_{\tau_i, \tau_j}^{f_m} \end{pmatrix} = \begin{pmatrix} 1 & \rho_{\tau_j}^{f_1} \\ 1 & \rho_{\tau_j}^{f_2} \\ \vdots & \vdots \\ 1 & \rho_{\tau_j}^{f_m} \end{pmatrix} \begin{pmatrix} c_0 \\ c_1 \end{pmatrix} + \begin{pmatrix} e_1 \\ e_2 \\ \vdots \\ e_m \end{pmatrix}, \quad (3)$$

$$\mu_{\tau_i, \tau_j}^{f_l} = E[\rho_{\tau_i, \tau_j}^{f_l}] = [1 \ \rho_{\tau_j}^{f_l}] \cdot [c_0 \ c_1]^\top, \quad (4)$$

$$\sigma_{\tau_i, \tau_j}^2 = var[\rho_{\tau_i, \tau_j}^{f_l}] = \frac{\sum_i e_i^2}{m}. \quad (5)$$

We assume that there are m frames prior to frame f_l in which tracks τ_i and τ_j were active simultaneously and the relative distances between them were recorded. c_0 and c_1 are the least-squares solutions to (3). Finally, the estimated locations $\rho_{\tau_i, \tau_j}^{f_l} | \tau_j \in kn(\tau_i)$ based on k neighbors are combined as follows (for simplicity we drop the superscript f_l):

$$\rho_{\tau_i} \sim \prod_{\tau_j \in kn(\tau_i)} \mathcal{N}(\mu_{\tau_i, \tau_j}, \sigma_{\tau_i, \tau_j}^2), \quad (6)$$

$$\sim \beta \mathcal{N}(\mu_{\tau_i}, \sigma_{\tau_i}^2), \quad (7)$$

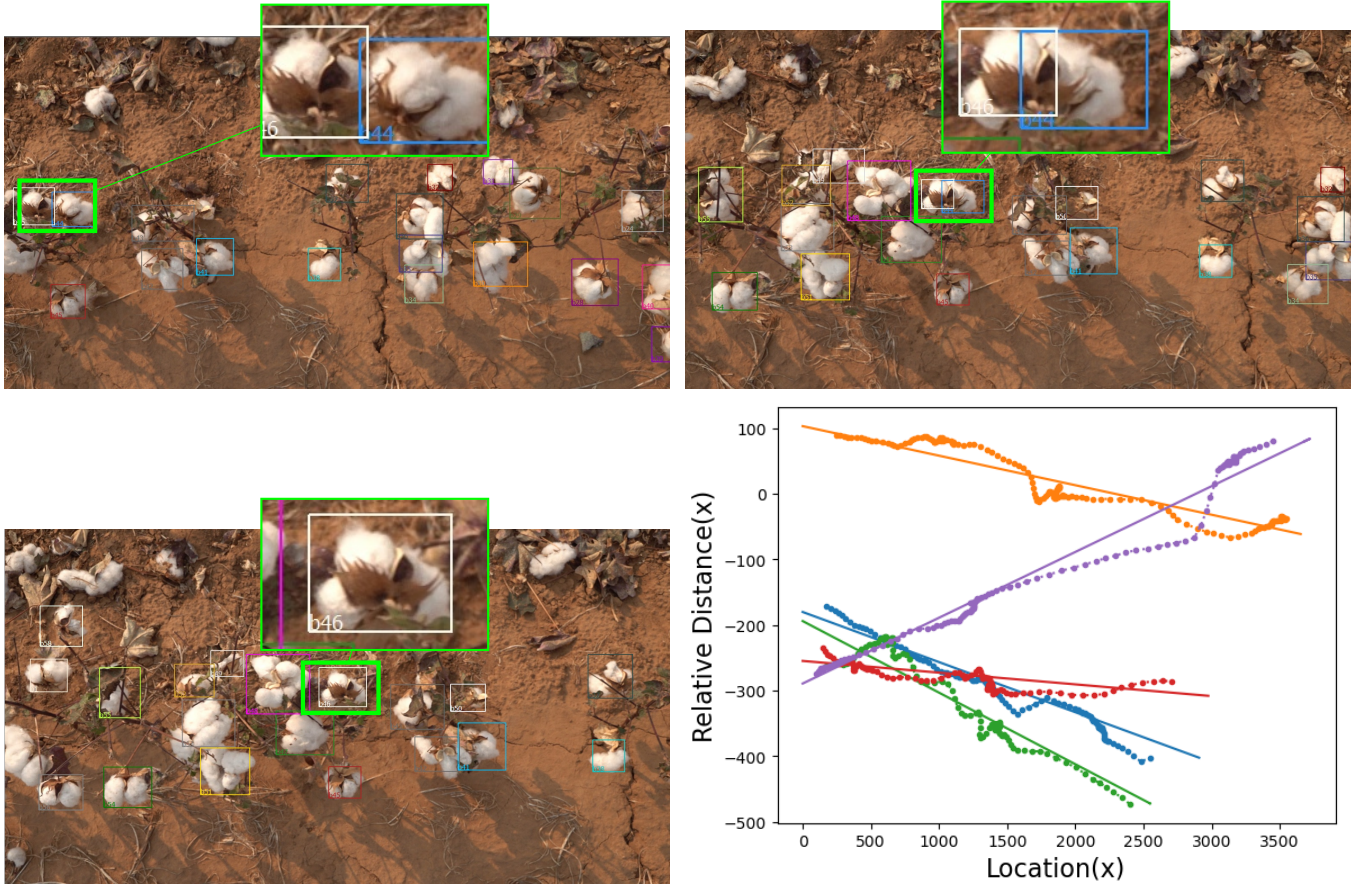


Fig. 5: The relative distance between neighboring cotton bolls changes gradually due to the shift in perspective. At frame 1142, the distance between *b46* and *b44* is large (top left). At frame 1203, the distance between the bolls reduces (top right). At frame 1212, both bolls overlap, i.e., the distance is zero (bottom left). The plot shows the relative distances between pairs of cotton bolls versus their locations (bottom right). The distance and location are measured in image coordinates along x (width) direction. Each dotted line shows the distance between a pair of cotton bolls. The straight lines are linear fits, for reference, to the respective dotted lines.

where β is a scaling factor and

$$\sigma_{\tau_i} = \left(\sum_{\tau_j \in kn(\tau_i)} \sigma_{\tau_i, \tau_j}^{-2} \right)^{-1/2}, \quad (8)$$

$$\mu_{\tau_i} = \sigma_{\tau_i}^2 \sum_{\tau_j \in kn(\tau_i)} \sigma_{\tau_i, \tau_j}^{-2} \mu_{\tau_i, \tau_j}. \quad (9)$$

In (6), $kn(\tau_i)$ is the set of τ_i 's neighbors with cardinality k , which is inspired by the Kalman filter's approach to combine the prior with an observation for an improved estimate. The simplification from (6) to (7) is due to [43].

The neighbors $kn(\cdot)$ are selected based on the k -nearest neighbors algorithm. We measure the distances between the bounding box centers using their Euclidean norm. For a particular track τ_i , we can end up with more than k neighbor locations in total, even if we record just k neighboring locations in each frame. In addition, we want to prioritize a neighbor that was simultaneously active with τ_i in more frames in the recent past. Therefore, to choose k neighbors among all the recorded neighbors we rank each neighbor,

$$R_{\tau_i}^{f_l}(\tau_j) = \sum_{f_m \in \mathcal{A}_{\tau_i, \tau_j}^{f_l}} f_m, \quad (10)$$

where $\mathcal{A}_{\tau_i, \tau_j}^{f_l}$ is the set of timestamps prior to f_l in which tracks τ_i and τ_j were active simultaneously. For example, suppose tracks τ_i and τ_{n_1} are simultaneously active at times 2, 3, and 5. Then, $\mathcal{A}_{\tau_i, \tau_{n_1}}^{f_l} = \{2, 3, 5\}$ and similarly $\mathcal{A}_{\tau_i, \tau_{n_2}}^{f_l} = \{5, 6\}$. In this case, we prioritize the neighbor n_2 according to the rank, which is higher than n_1 since $R_{\tau_i}^{f_l}(\tau_{n_2}) = 5 + 6 > R_{\tau_i}^{f_l}(\tau_{n_1}) = 2 + 3 + 5$.

IV. COTTON BOLL DATASET

A. Video Acquisition Details

To construct the **TexCot22** [11] dataset we captured multiple video sequences for training and testing. Similar to other tracking datasets, each tracking sequence is 10 to 20 seconds in length. The dataset consists of a total of 30 sequences of which 17 are for training and the remaining 13 are for testing.

The video sequences were captured at 4K resolution and at distinct frame rates (e.g., 10, 15, 30). There are typically 2 to 10 cotton bolls per cluster. The average width and height of an annotated bounding box is approximately 230×210 pixels.

To make the dataset robust to environmental conditions, we recorded the field videos at separate times of day to account for varying lighting conditions. In total, there are roughly 30×300

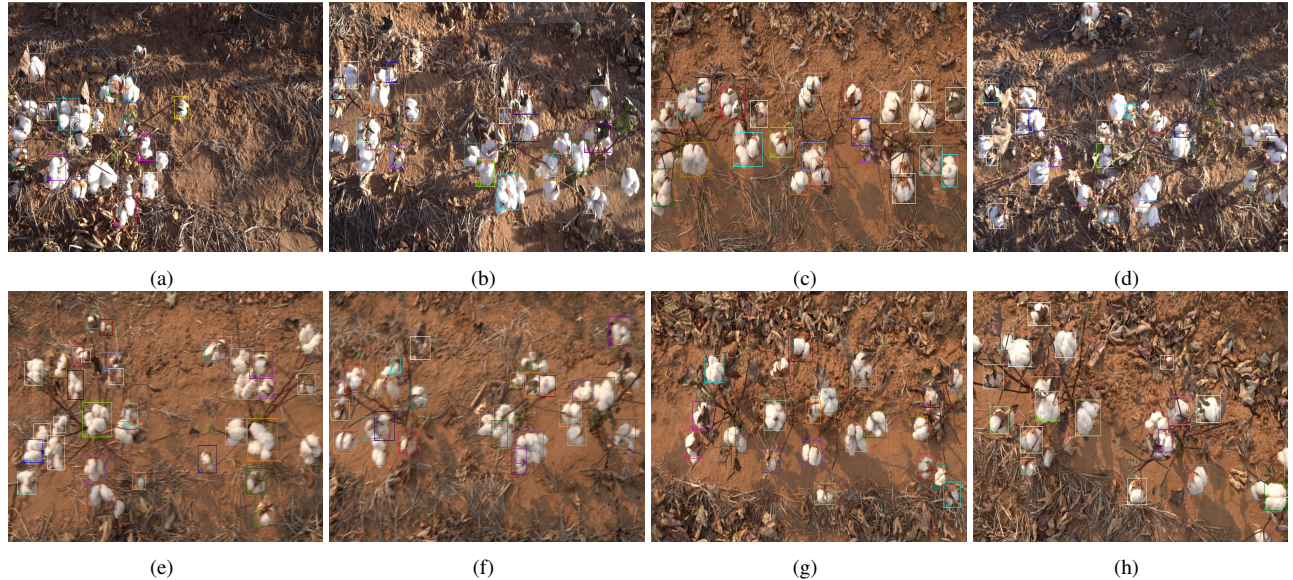


Fig. 6: Examples (a-h) of annotated cotton boll field images with complex backgrounds from the **TexCot22** [11] dataset.

	Rule
What	Any open cotton bolls on plants excluding bolls that have fallen to the ground.
When	Start when the enclosing bounding box enters the frame. Remove as soon as the bounding box goes beyond the frame border.
How	Annotations are not pixel perfect. The majority of pixels belonging to a cotton boll should be contained by the bounding box.
Occlusion	Annotate a cotton boll as long as it is partially visible and distinguishable from the neighboring bolls. In the case of a long occlusion interval, the same ID is assigned to the occluded boll as long as it is identifiable.

TABLE I: The annotation rules used for constructing the **TexCot22** [11] dataset.

frames with 150,000 labeled instances. On average there are 70 unique cotton bolls in each sequence.

The directory structure of the dataset is similar to MOT17 [44]. The ground truth and the detection files are also available in MOT17 format. Hence, any tracking method that runs on MOT17 can readily utilize **TexCot22** without any additional modifications. Example ground-truth images from the dataset are displayed in Fig. 6.

B. Annotation Rules

We followed a set of rules to exhaustively annotate all cotton bolls in each sequence with bounding boxes. The bounding boxes around the cotton bolls are very tight, however there may exist some pixels outside of the bounding box that are part of the boll. A compiled a set of annotation rules is provided in Table I.

V. EXPERIMENTS

A. Implementation Details

To make a fair comparison among existing tracking methods, we generated the same set of detection bounding boxes

utilizing a Cascade R-CNN [45] model with a ResNet-50 backbone. Using the **TexCot22** training data, the model was trained for 100 epochs. The training took place on a CentOS 7.6.1810 machine using an Intel Xeon E5-2620 2.10 GHz CPU, 132 GB of memory, and an NVIDIA GeForce GTX 1080 Ti GPU. The detection accuracy of the trained model was 97% on the test data. We also tried the detector provided by the official Tracktor [16] GitHub repository. However, our detector achieved the best results among all the trackers.

For calculating dense optical flow, we made use of the OpenCV [46] implementation of the Gunnar-Farneback algorithm. The estimated flow velocity of a bounding box is computed by averaging the velocities of the center pixels (e.g., a 3×3 window at the bounding box center). The problem of assigning the set of detected bounding boxes to the set of predicted bounding boxes is solved via ByteTrack’s [19] association procedure.

To estimate the relative location based on the k -nearest neighbors, we empirically opted for a neighbor size of three. If we considered too many neighbors, then the RLA module gave a coarse relative location. Conversely, a single neighbor often provided a noisy estimation. The relative locations along the x (width) and y (height) directions were calculated independently using (7).

B. Cotton Boll Tracking Evaluation

We evaluated multiple MOT metrics including higher order tracking accuracy (HOTA) [47], identity-aware [48], and those defined by CLEAR MOT [49]. Association and localization are two major criteria for deciding tracking performance. While measures such as MOTA (accuracy) and MOTP (precision) emphasize localization, the IDP (identification precision), IDR (identification recall), IDF₁ (identification F_1 score), and IDsw (identity switches) put more weight on maintaining true identity. The Frag (fragmentation) metric is the number of times an object is lost, but then redetected

Method	IDP \uparrow	IDR \uparrow	IDF $_1\uparrow$	HOTA \uparrow	MOTA \uparrow	MOTP \uparrow	IDsw \downarrow	Frag \downarrow
DeepSORT	82.50%	81.97%	82.24%	66.47%	84.80%	80.07%	1751	633
Tracktor	82.47%	81.01%	81.74%	66.28%	86.56%	79.03%	2070	787
ByteTrack	90.88%	88.76%	89.80%	71.19%	88.60%	80.32%	1193	564
TrackFormer	89.94%	70.40%	78.98%	54.90%	69.58%	70.86%	652	311
NTrack (ours)	93.28%	91.70%	92.49%	73.56%	89.25%	81.49%	1062	508

TABLE II: A comparison of NTrack against DeepSORT [6], Tracktor [16], ByteTrack [19], and TrackFormer [29]. The arrow directions indicate the optimal metric values.

Method	MAPE \downarrow	RMSE \downarrow
Deep learning [40]	9.00%	9.00 (best case)
Geometric-feature-based [39]	15.04%	7.40
3D point cloud-based [41]	10.00%	16.87
NTrack (ours)	4.00%	4.73

TABLE III: Cotton boll counting error.

in a future frame thus fragmenting the track. The evaluation was performed against the following state-of-the-art tracking methods: DeepSORT [6], Tracktor [16], ByteTrack [19], and Trackformer [29]. As shown in Table II, NTrack outperforms these systems by a significant margin in the majority of the metrics.

Our primary goal was to design a tracking system that can count cotton bolls with high accuracy. Thus, by design NTrack should perform better in ID preserving performance metrics. Nevertheless, our tracker outperforms other methods in localization measures as well. In addition, NTrack demonstrates its overall superiority by exceeding others in the HOTA measure, which explicitly balances the effect of performing accurate detection, association, and localization into a single unified metric. To avoid data labeling inconsistencies near the frame border, we considered the ground truth and hypothesis bounding boxes that do not overlap with the frame margin. More specifically, we consider 200 pixels on both sides of a frame as the margin.

C. Cotton Boll Counting Evaluation

Determining the number of unique cotton bolls in a given video sequence was a prime requirement in designing NTrack. Therefore, when creating the tracker we focused on maintaining the true identity of the bolls. As shown in Table III, the counting results show that NTrack performs exceptionally well at the counting task when compared to other cotton boll counting methods. These results are based on the mean absolute percentage error (MAPE) and root mean square error (RMSE), which are defined as

$$\text{MAPE} = \frac{1}{n} \sum_{i=1}^n \frac{|C_{gt} - C_h|}{C_{gt}}, \quad (11)$$

$$\text{RMSE} = \sqrt{\frac{1}{n} \sum_{i=1}^n (C_{gt} - C_h)^2}. \quad (12)$$

In (11) and (12), C_{gt} and C_h are the number of unique cotton bolls detected manually (i.e., the ground truth) and by NTrack in the i th video sequence, respectively, and n is the number of video sequences. The results reported for the other methods in Table III are taken from their respective papers since the datasets and source code are not publicly available.

Table IV shows the performance of NTrack against state-of-the-art tracking techniques. The results in Table IV were obtained from experiments done with the same test dataset (TexCot22) and protocol. NTrack outperformed all of the other methods. It is interesting to note that TrackFormer, which is based on a transformer architecture, was able to track cotton bolls more consistently than NTrack in terms of ID switching and fragmentation (Table II). Nevertheless, TrackFormer’s counting error (8%) is twice that of NTrack (4%).

To demonstrate that the difference in counting performance reported in Table IV is statistically significant, we conducted hypothesis testing. Specifically, we performed one-sided paired t-tests against the other tracking techniques. The null hypothesis of the test is the assumption that the mean counting error of NTrack is greater than or equal to other methods, i.e.,

$$H_0 : \mu_n \geq \mu_x. \quad (13)$$

Conversely, the alternative hypothesis is the assumption that the mean counting error of NTrack is less than the other methods, i.e.,

$$H_a : \mu_n < \mu_x. \quad (14)$$

In (13) and (14), μ_n and μ_x are the mean counting errors of NTrack and the other techniques (e.g., DeepSORT, Tracktor, ByteTrack, and TrackFormer), respectively. The test results (p-values) in Table V demonstrate that we can reject the null hypothesis at a significance level of $\alpha = 0.05$ in favor of the alternative hypothesis. In other words, with 95% confidence we can conclude that the test data provides sufficient evidence to support the observation that NTrack’s mean counting error is lower than the other methods.

D. Qualitative Evaluation

We conducted a qualitative analysis of NTrack against the trackers in the evaluation set. The first two rows, from the top of Fig. 7, show the tracking outcomes of NTrack and DeepSORT on a test video sequence. In row 2, the arrow highlights the track of a specific cotton boll with an ID of 83. DeepSORT fails to track this boll between frame 122 and frame 177 as indicated by the red arrow. At frame 177, DeepSORT cannot reidentify the previously seen cotton boll (ID 83) and it erroneously assigns a new ID (ID 142). Similarly, Tracktor (row 3, ID 57), and ByteTrack (row 4, ID 60) also fail to track the same cotton boll. TrackFormer (row 5) does not even detect the cotton boll in frames 80 and 122. However, NTrack (row 1) successfully tracks this boll (ID 33) and assigns the same ID in frame 177.

Sequence	GT	NTrack (ours)		DeepSORT		Tracktor		ByteTrack		TrackFormer	
		Count	Error %	Count	Error %	Count	Error %	Count	Error %	Count	Error %
vid09_01	66	66	0	115	74	220	233	77	17	58	12
vid09_02	72	80	11	146	103	234	225	90	25	74	3
vid09_03	72	67	4	105	46	208	189	78	8	62	14
vid14_01	95	102	7	233	145	396	317	123	29	103	8
vid23_01	60	56	7	136	127	187	212	93	55	57	5
vid23_02	50	46	8	64	28	136	172	52	4	49	2
vid23_03	96	95	1	140	46	223	132	101	5	88	8
vid25_01	68	67	1	80	18	119	75	72	5	64	6
vid25_02	73	72	1	103	41	184	152	88	21	57	22
vid25_03	61	60	2	69	10	111	10	62	2	62	2
vid26_01	51	51	0	86	69	134	163	60	18	53	4
vid26_02	66	67	1	79	20	120	82	69	5	59	11
vid26_03	66	69	5	82	24	126	91	71	8	71	8
Mean Error			4		55		163		15		8

TABLE IV: The accuracy of NTrack against DeepSORT [6], Tracktor [16], ByteTrack [19], and TrackFormer [29] is shown by comparing the ground truth (GT) cotton boll counts with the estimated counts.

	ByteTrack	DeepSORT	Tracktor	TrackFormer
NTrack	0.003945	0.001769	0.000027	0.033470

TABLE V: The hypothesis testing results on the mean cotton boll counting error. For each column, we report the test result between NTrack and the competing method in terms of the p-value.

Method	Linear motion	Dynamic motion	RLA	IDF ₁ ↑	MOTA↑	IDsw↓
Baseline	✓			90.3	88.9	3682
NTrack_motion		✓		92.2	89.3	264
NTrack_N1		✓	✓	92.5	89.5	101
NTrack_N3		✓	✓	92.8	89.5	85
NTrack_N5		✓	✓	92.8	89.4	85

TABLE VI: A comparison of the impact of integrating different modules into NTrack against a ByteTrack [19] baseline. NTrack_N1, NTrack_N3, NTrack_N5 model use 1, 3, and 5 neighbors respectively, in the RLA module.

Fig. 8 shows additional qualitative tracking results in a more challenging scenario involving wind. In this scene, a cotton boll (ID 4 in rows 1, 2, 4, ID 7 in row 3, ID 17 in row 5) is occluded for an extended period after frame 54. When the cotton boll reappears in frame 113, it is successfully reidentified by NTrack (row 1). In contrast, DeepSORT and ByteTrack assign a new ID (ID 123 and ID 69 in rows 2 and 4, respectively) to the boll. Tracktor and TrackFormer are unable to detect the cotton boll (rows 3 and 5, respectively). These observations demonstrate the effectiveness of our tracking system in reidentifying cotton bolls, especially in the field under harsh environmental conditions.

We also qualitatively evaluated NTrack by way of visual appearance-based re-identification of cotton bolls across a video sequence. Examples where appearance-based re-identification fails are shown in Fig. 9. The similarity scores in Fig. 9 are calculated using the cosine similarity between a pair of appearance descriptors (r_i, r_j) [6]. Concretely,

$$\text{cosine similarity}(r_i, r_j) = \frac{r_i^\top r_j}{\|r_i\| \cdot \|r_j\|}, \quad (15)$$

where $\|r_i\| = \|r_j\| = 1$. (15) outputs a real number in the range $[0, 1]$. Identical cotton bolls have a cosine similarity score of 1, while distinct bolls have a score of 0.

In the **TexCot22** dataset, we hypothesize that all tracking methods that depend on visual appearance to reidentify objects after reappearing will fail to maintain true identity. This is based on the observation that re-identification techniques exploited by many popular tracking methods (e.g., [50]) tend to differentiate objects using color and shape as distinctive features. However, individual cotton bolls have a homogeneous color and shape distribution. Furthermore, the appearance of a cotton boll changes drastically due to the shift in perspective after being occluded for a few frames. Even for an experienced

human, it is challenging to reidentify these reappearing cotton bolls. Nevertheless, NTrack can successfully reidentify the bolls (i.e., assign the same ID).

E. Ablation Study

To analyze our system design choices, we decoupled and validated the performance impact of each of NTrack’s modules. Table VI shows the contributions of the various modules when compared against a ByteTrack [19] baseline. The overall performance of NTrack gradually improved upon integrating each module. The baseline system uses a Kalman filter for motion prediction and an effective association method to reidentify objects. When compared to the baseline, our dynamic motion model improved the IDF₁ score by 2%. The combined model, *NTrack_motion* (baseline + dynamic motion model), also reduced the counting error by a large amount. This supports the hypothesis that for small objects (e.g., fruits, flowers, etc.) that move irregularly in the wild, a dynamic motion model is preferable for tracking.

We designed the RLA module specifically for identifying occluded cotton bolls. Our experiments show that the RLA module serves its purpose very well. In particular, NTrack achieved the highest scores on the IDF₁, MOTA, and IDsw metrics when the RLA module was combined with the dynamic motion model. Although there was only a 0.6% gain in the IDF₁ score due to the addition of the RLA module, the improvement is significant since there are few occluded bolls in a video sequence when compared to the total number of bolls. The number of neighbors (e.g., 1, 3, or 5) in the RLA module was empirically selected for these experiments.

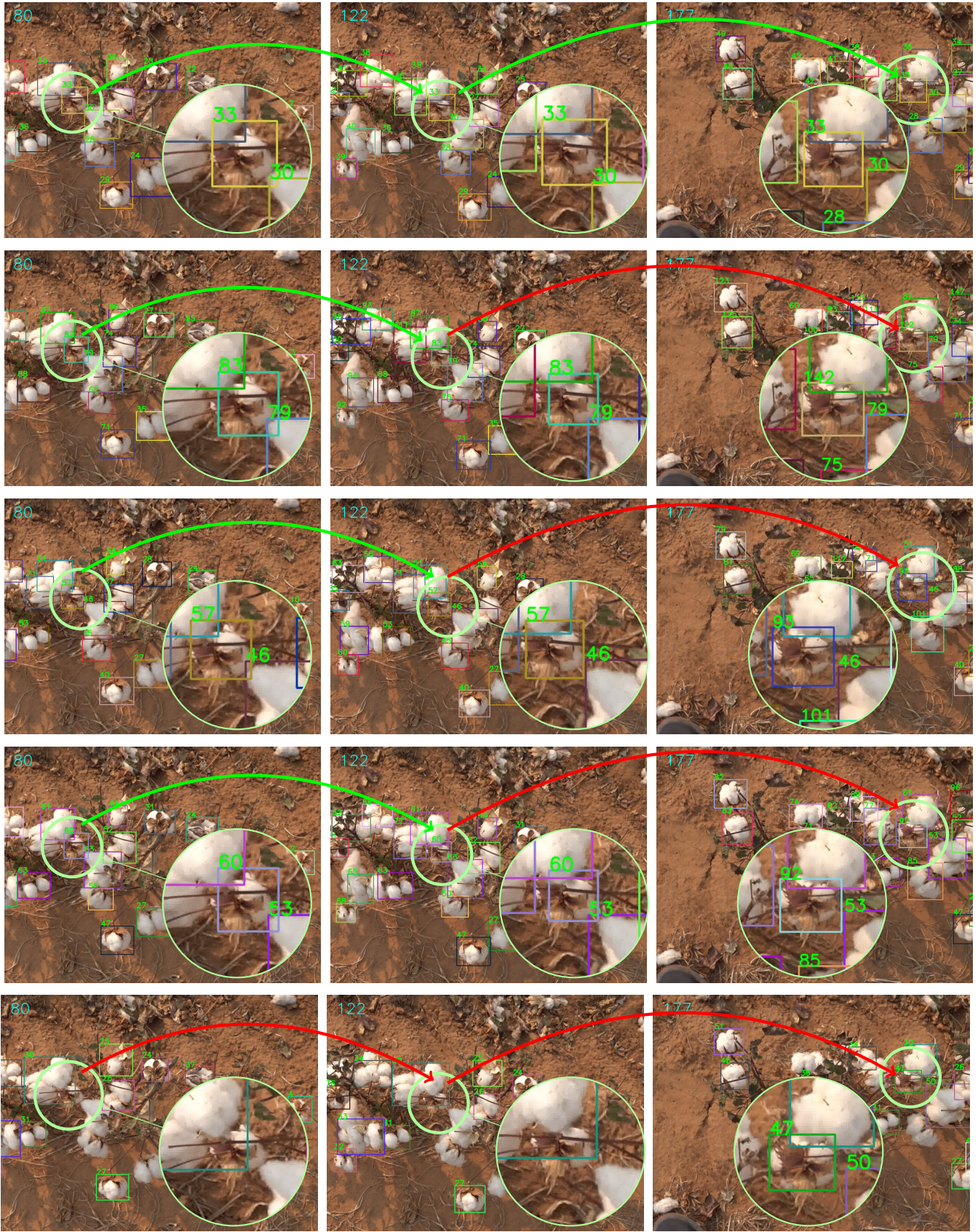


Fig. 7: The first scenario qualitative comparison between NTrack and the competing methods on the **TexCot22** [11] dataset. From top to bottom, each row (NTrack, DeepSORT [6], Tractor [16], ByteTrack [19], and Trackformer [29]) shows the tracking performance of the different techniques on the same video sequence. The numbers (80, 122, 177) at the top-left corner of each image portray the frame number in the corresponding video sequence. Correct and incorrect associations between cotton bolls are illustrated by the green and red arrows, respectively. The numbers at the top-left corner of each bounding box report the identity of the associated cotton boll assigned by the tracker.

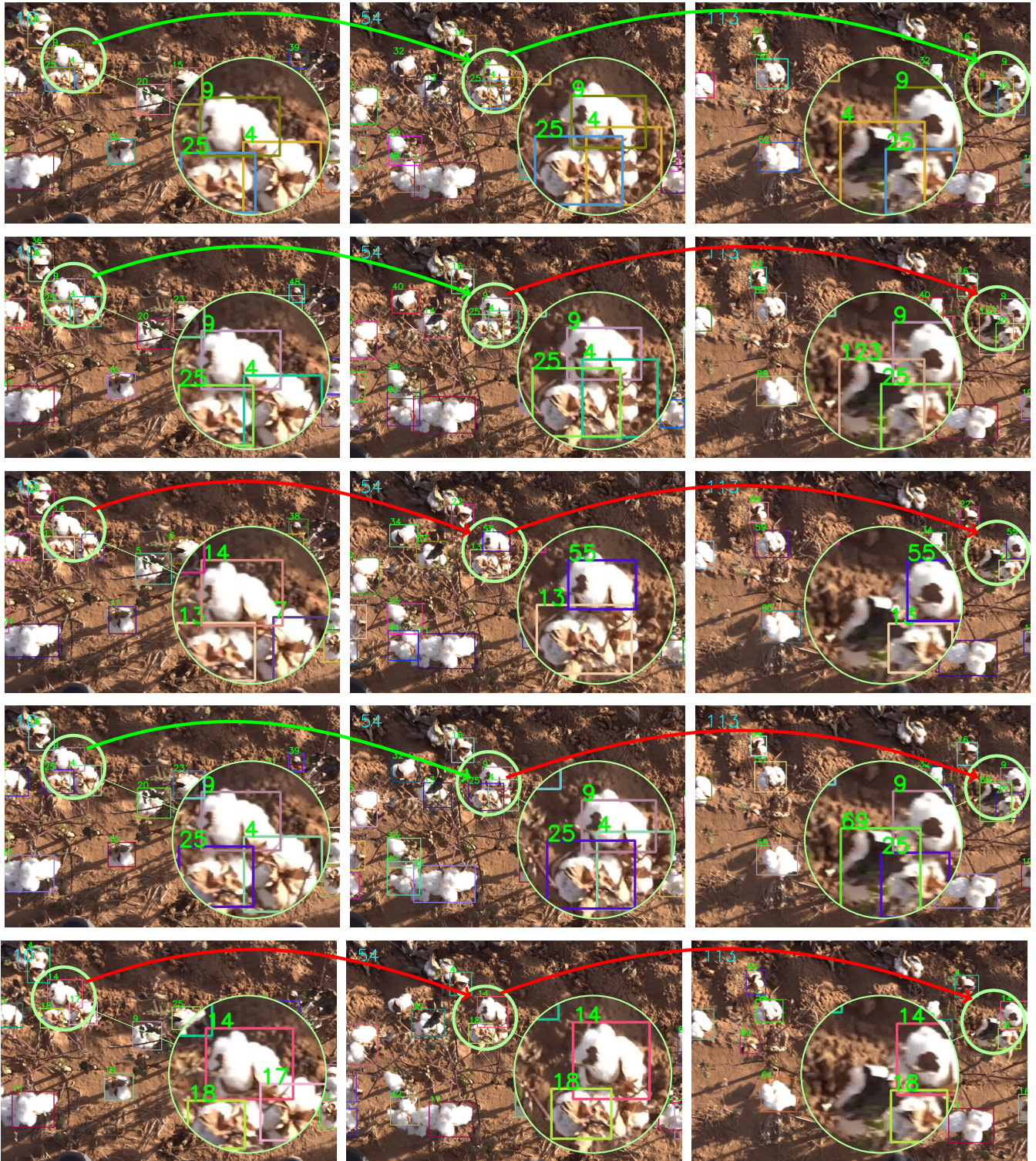


Fig. 8: The second scenario qualitative comparison between NTrack and the competing methods on the **TexCot22** [11] dataset. From top to bottom, each row (NTrack, DeepSORT [6], Tractor [16], ByteTrack [19], and Trackformer [29]) shows the tracking performance of the different techniques on the same video sequence. The numbers (10, 54, 133) at the top-left corner of each image portray the frame number in the corresponding video sequence. Correct and incorrect associations between cotton bolls are illustrated by the green and red arrows, respectively. The numbers at the top-left corner of each bounding box report the identity of the associated cotton boll assigned by the tracker.

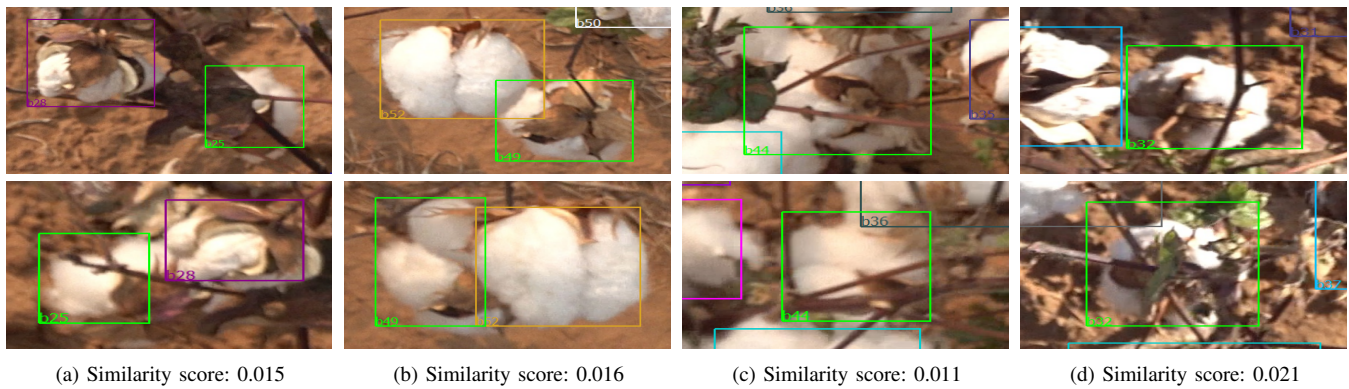


Fig. 9: NTrack re-identification results. Each column shows the same set of cotton bolls. The bottom row shows the bolls after being occluded for several frames. The bounding box colors represent the *true* identity of the objects and the IDs (e.g., b25, b49, etc.) at the bottom left corner of the bounding boxes are *assigned* by NTrack. To highlight the poor performance of visual similarity, each column is accompanied with a cosine similarity score calculated between the *green* bounding boxes. The correspondences between the bounding box colors and IDs illustrates that NTrack can successfully reidentify cotton bolls without visual similarity.

VI. CONCLUSION

In this paper we described NTrack, a relative location-based MOT system that enables accurate tracking of cotton bolls in outdoor field environments. NTrack is able to robustly maintain object identity and it can reidentify objects after long periods of occlusion, which is a common scenario in agricultural applications. What’s more, we introduced **TexCot22**, the *first* infield cotton boll video dataset. Using this dataset, NTrack was evaluated against other contemporary MOT techniques and shown to significantly outperform all of them in identity preserving metrics. In future work, we will extend our framework to incorporate multiple view tracking data in order to further improve the automated counting of infield cotton bolls.

ACKNOWLEDGMENTS

The data collected for the research results reported within this paper was done in collaboration with Texas Tech University and the Texas A&M AgriLife Research and Extension Center’s Halfway Station. The authors acknowledge the Texas Advanced Computing Center (TACC) at The University of Texas at Austin for providing software, computational, and storage resources that have contributed to these results.

REFERENCES

- [1] USDA-ERS-1, “Cotton & wool overview,” 2023, available Online: <https://www.ers.usda.gov/topics/crops/cotton-wool/>.
- [2] National Cottonseed Products Association, 2023, available Online: <https://www.cottonseed.com/>.
- [3] M. Reynolds and P. Langridge, “Physiological breeding,” *Current Opinion in Plant Biology*, vol. 31, pp. 162–171, 2016.
- [4] X. Zhou, B. English, C. Boyer, R. Roberts, J. Larson, D. Lambert, M. Velandia, L. Falconer, S. Martin, K. Larkin, K. Paudel, A. Mishra, R. Rejesus, C. Wang, S. E. and J. Reeves, “Precision farming by cotton producers in fourteen southern states: Results from the 2013 southern cotton farm survey,” *Research Series*, pp. 15–001, 2015.
- [5] F. Yu, W. Li, Q. Li, Y. Liu, X. Shi, and J. Yan, “Poi: Multiple object tracking with high performance detection and appearance feature,” in *Proceedings of the European Conference on Computer Vision*. Springer, 2016, pp. 36–42.
- [6] N. Wojke, A. Bewley, and D. Paulus, “Simple online and realtime tracking with a deep association metric,” in *Proceedings of the IEEE International Conference on Image Processing*, 2017, pp. 3645–3649.
- [7] Z. Wang, L. Zheng, Y. Liu, Y. Li, and S. Wang, “Towards real-time multi-object tracking,” in *Proceedings of the European Conference on Computer Vision*. Springer, 2020, pp. 107–122.
- [8] D. Koller, J. Weber, and J. Malik, “Robust multiple car tracking with occlusion reasoning,” in *Proceedings of the European Conference on Computer Vision*. Springer, 1994, pp. 189–196.
- [9] M. Betke, E. Haritaoglu, and L. S. Davis, “Real-time multiple vehicle detection and tracking from a moving vehicle,” *Machine Vision and Applications*, vol. 12, no. 2, pp. 69–83, 2000.
- [10] J. R. Mauney, “Vegetative growth and development of fruiting sites,” *Cotton Physiology*, pp. 11–28, 1986.
- [11] M. A. Al Muzaddid and W. J. Beksi, “Texcot22,” 2023. [Online]. Available: <https://doi.org/10.18738/T8/5M9NCI>
- [12] W. Luo, J. Xing, A. Milan, X. Zhang, W. Liu, and T.-K. Kim, “Multiple object tracking: A literature review,” *Artificial Intelligence*, vol. 293, p. 103448, 2021.
- [13] L. Zhang, Y. Li, and R. Nevatia, “Global data association for multi-object tracking using network flows,” in *Proceedings of the IEEE/CVF Conference on Computer Vision and Pattern Recognition*, 2008, pp. 1–8.
- [14] C. Huang, B. Wu, and R. Nevatia, “Robust object tracking by hierarchical association of detection responses,” in *Proceedings of the European Conference on Computer Vision*. Springer, 2008, pp. 788–801.
- [15] B. Yang, C. Huang, and R. Nevatia, “Learning affinities and dependencies for multi-target tracking using a crf model,” in *Proceedings of the IEEE/CVF Conference on Computer Vision and Pattern Recognition*, 2011, pp. 1233–1240.
- [16] P. Bergmann, T. Meinhardt, and L. Leal-Taixé, “Tracking without bells and whistles,” in *Proceedings of the IEEE/CVF International Conference on Computer Vision*, 2019, pp. 941–951.
- [17] G. Brasó and L. Leal-Taixé, “Learning a neural solver for multiple object tracking,” in *Proceedings of the IEEE/CVF Conference on Computer Vision and Pattern Recognition*, 2020, pp. 6247–6257.
- [18] Y. Zhang, C. Wang, X. Wang, W. Zeng, and W. Liu, “Fairmot: On the fairness of detection and re-identification in multiple object tracking,” *International Journal of Computer Vision*, vol. 129, no. 11, pp. 3069–3087, 2021.
- [19] Y. Zhang, P. Sun, Y. Jiang, D. Yu, F. Weng, Z. Yuan, P. Luo, W. Liu, and X. Wang, “Bytetrack: Multi-object tracking by associating every detection box,” in *Proceedings of the European Conference on Computer Vision*. Springer, 2022, pp. 1–21.
- [20] L. Leal-Taixé, M. Fenzi, A. Kuznetsova, B. Rosenhahn, and S. Savarese, “Learning an image-based motion context for multiple people tracking,” in *Proceedings of the IEEE/CVF Conference on Computer Vision and Pattern Recognition*, 2014, pp. 3542–3549.
- [21] A. Bewley, Z. Ge, L. Ott, F. Ramos, and B. Upcroft, “Simple online and realtime tracking,” in *Proceedings of the IEEE International Conference on Image Processing*, 2016, pp. 3464–3468.
- [22] H. W. Kuhn, “The hungarian method for the assignment problem,” *Naval Research Logistics Quarterly*, vol. 2, no. 1-2, pp. 83–97, 1955.
- [23] K. Okuma, A. Taleghani, N. d. Freitas, J. J. Little, and D. G. Lowe, “A boosted particle filter: Multitarget detection and tracking,” in *Proceed-*

- ings of the *European Conference on Computer Vision*. Springer, 2004, pp. 28–39.
- [24] Y. Li, H. Ai, T. Yamashita, S. Lao, and M. Kawade, “Tracking in low frame rate video: A cascade particle filter with discriminative observers of different life spans,” *IEEE Transactions on Pattern Analysis and Machine Intelligence*, vol. 30, no. 10, pp. 1728–1740, 2008.
- [25] W. Choi, “Near-online multi-target tracking with aggregated local flow descriptor,” in *Proceedings of the IEEE/CVF International Conference on Computer Vision*, 2015, pp. 3029–3037.
- [26] J. H. Yoon, M.-H. Yang, J. Lim, and K.-J. Yoon, “Bayesian multi-object tracking using motion context from multiple objects,” in *Proceedings of the IEEE/CVF Winter Conference on Applications of Computer Vision*, 2015, pp. 33–40.
- [27] A. Mauri, R. Khemmar, B. Decoux, N. Rago, R. Rossi, R. Trabelsi, R. Boutteau, J.-Y. Ertaud, and X. Savatier, “Deep learning for real-time 3d multi-object detection, localisation, and tracking: Application to smart mobility,” *Sensors*, vol. 20, no. 2, p. 532, 2020.
- [28] C. Godard, O. Mac Aodha, M. Firman, and G. J. Brostow, “Digging into self-supervised monocular depth estimation,” in *Proceedings of the IEEE/CVF International Conference on Computer Vision*, 2019, pp. 3828–3838.
- [29] T. Meinhardt, A. Kirillov, L. Leal-Taixé, and C. Feichtenhofer, “Trackerformer: Multi-object tracking with transformers,” in *Proceedings of the IEEE/CVF Conference on Computer Vision and Pattern Recognition*, 2022, pp. 8844–8854.
- [30] F. Porikli, O. Tuzel, and P. Meer, “Covariance tracking using model update based on lie algebra,” in *Proceedings of the IEEE/CVF Conference on Computer Vision and Pattern Recognition*, vol. 1, 2006, pp. 728–735.
- [31] D. Mitzel and B. Leibe, “Real-time multi-person tracking with detector assisted structure propagation,” in *Proceedings of the IEEE/CVF International Conference on Computer Vision Workshops*, 2011, pp. 974–981.
- [32] W. Choi and S. Savarese, “A unified framework for multi-target tracking and collective activity recognition,” in *Proceedings of the European Conference on Computer Vision*. Springer, 2012, pp. 215–230.
- [33] C. Hung, J. Underwood, J. Nieto, and S. Sukkarieh, “A feature learning based approach for automated fruit yield estimation,” in *Field and Service Robotics*. Springer, 2015, pp. 485–498.
- [34] S. W. Chen, S. S. Shivakumar, S. Dcunha, J. Das, E. Okon, C. Qu, C. J. Taylor, and V. Kumar, “Counting apples and oranges with deep learning: A data-driven approach,” *IEEE Robotics and Automation Letters*, vol. 2, no. 2, pp. 781–788, 2017.
- [35] P. Roy and V. Isler, “Surveying apple orchards with a monocular vision system,” in *Proceedings of the IEEE International Conference on Automation Science and Engineering*, 2016, pp. 916–921.
- [36] N. Häni, P. Roy, and V. Isler, “Apple counting using convolutional neural networks,” in *Proceedings of the IEEE/RSJ International Conference on Intelligent Robots and Systems*, 2018, pp. 2559–2565.
- [37] M. Afonso, H. Fonteijn, F. S. Fiorentin, D. Lensink, M. Mooij, N. Faber, G. Polder, and R. Wehrens, “Tomato fruit detection and counting in greenhouses using deep learning,” *Frontiers in Plant Science*, p. 1759, 2020.
- [38] R. Kirk, M. Mangan, and G. Cielniak, “Robust counting of soft fruit through occlusions with re-identification,” in *Proceedings of the International Conference on Computer Vision Systems*. Springer, 2021, pp. 211–222.
- [39] S. Sun, C. Li, A. H. Paterson, P. W. Chee, and J. S. Robertson, “Image processing algorithms for infield single cotton boll counting and yield prediction,” *Computers and Electronics in Agriculture*, vol. 166, p. 104976, 2019.
- [40] D. Tedesco-Oliveira, R. P. da Silva, W. Maldonado Jr, and C. Zerbato, “Convolutional neural networks in predicting cotton yield from images of commercial fields,” *Computers and Electronics in Agriculture*, vol. 171, p. 105307, 2020.
- [41] S. Sun, C. Li, P. W. Chee, A. H. Paterson, Y. Jiang, R. Xu, J. S. Robertson, J. Adhikari, and T. Shehzad, “Three-dimensional photogrammetric mapping of cotton bolls in situ based on point cloud segmentation and clustering,” *ISPRS Journal of Photogrammetry and Remote Sensing*, vol. 160, pp. 195–207, 2020.
- [42] G. Farneäck, “Two-frame motion estimation based on polynomial expansion,” in *Proceedings of the Scandinavian Conference on Image Analysis*. Springer, 2003, pp. 363–370.
- [43] P. Bromiley, “Products and convolutions of gaussian probability density functions,” *Tina-Vision Memo*, vol. 3, no. 4, p. 1, 2003.
- [44] A. Milan, L. Leal-Taixé, I. Reid, S. Roth, and K. Schindler, “Mot16: A benchmark for multi-object tracking,” *arXiv preprint arXiv:1603.00831*, 2016.
- [45] Z. Cai and N. Vasconcelos, “Cascade r-cnn: Delving into high quality object detection,” in *Proceedings of the IEEE/CVF Conference on Computer Vision and Pattern Recognition*, 2018, pp. 6154–6162.
- [46] G. Bradski, “The opencv library,” *Dr. Dobbs’ Journal: Software Tools for the Professional Programmer*, vol. 25, no. 11, pp. 120–123, 2000.
- [47] J. Luiten, A. Osep, P. Dendorfer, P. Torr, A. Geiger, L. Leal-Taixé, and B. Leibe, “Hota: A higher order metric for evaluating multi-object tracking,” *International Journal of Computer Vision*, vol. 129, no. 2, pp. 548–578, 2021.
- [48] E. Ristani, F. Solera, R. Zou, R. Cucchiara, and C. Tomasi, “Performance measures and a data set for multi-target, multi-camera tracking,” in *Proceedings of the European Conference on Computer Vision*. Springer, 2016, pp. 17–35.
- [49] K. Bernardin and R. Stiefelhagen, “Evaluating multiple object tracking performance: the clear mot metrics,” *EURASIP Journal on Image and Video Processing*, vol. 2008, pp. 1–10, 2008.
- [50] N. Wojke and A. Bewley, “Deep cosine metric learning for person re-identification,” in *Proceedings of the IEEE/CVF Winter Conference on Applications of Computer Vision*, 2018, pp. 748–756.



Md Ahmed Al Muzaddid received the B.S. degree in computer science and engineering from the Bangladesh University of Engineering and Technology. He is currently pursuing the Ph.D. degree with the Department of Computer Science and Engineering, The University of Arlington at Texas. His research interests include computer vision, machine learning, and agricultural automation.



William J. Beks (Member, IEEE) received the B.S. degree in mathematics and computer science from Stevens Institute of Technology in 2002, and the M.S. and Ph.D. degrees from the University of Minnesota in 2016 and 2018, respectively. He is currently an Assistant Professor in the Department of Computer Science and Engineering at The University of Arlington at Texas, where he also leads the Robotic Vision Laboratory. His research interests include robot perception, human-robot interaction, and autonomous systems.